

Self-starting self-similar all-polarization maintaining Yb-doped fiber laser

C. K. Nielsen¹, B. Ortaç, T. Schreiber, J. Limpert

Friedrich-Schiller-Universität Jena, Institute of Applied Physics, Jena, Germany.

¹also with Department of Physics, University of Aarhus, Denmark.

ckn@phys.au.dk

jens.limpert@uni-jena.de

R. Hohmuth², W. Richter^{2,3}

²*Friedrich-Schiller-Universität Jena, Institut of Solid State Physics, Jena, Germany.*

³*BATOP GmbH, Theodor-Körner Str. 4, 99425 Weimar, Germany.*

A. Tünnermann

Friedrich-Schiller-Universität Jena, Institute of Applied Physics, Jena, Germany

and

Fraunhofer Institute for Applied Optics and Precision Engineering, Jena, Germany

Abstract: We report on the generation of self-similar pulses from an self-starting saturable absorber mirror (SAM) based environmentally stable fiber laser comprising only polarization maintaining (PM) fibers. Pulse energies of 1 nJ at a repetition rate of 17 MHz were obtained, which could be externally compressed to an autocorrelation width of 280 fs.

© 2005 Optical Society of America

OCIS codes: (140.3510) Lasers, fiber; (140.4050) Mode-locked lasers.

References and links

1. M. E. Fermann, V. I. Kruglov, B. C. Thomsen, J. M. Dudley, and J. D. Harvey, "Self-Similar Propagation and Amplification of Parabolic Pulses in Optical Fibers," *Phys. Rev. Lett.* **84**, 6010–6013 (2000).
2. J. Limpert, T. Schreiber, T. Clausnitzer, K. Zöllner, H.-J. Fuchs, E.-B. Kley, H. Zellmer, and A. Tünnermann, "High-power femtosecond Yb-doped fiber amplifier," *Opt. Express* **10**, 628–638 (2002), <http://www.opticsexpress.org/abstract.cfm?URI=OPEX-10-14-628>.
3. V. I. Kruglov, A. C. Peacock, and J. D. Harvey, "Self-similar propagation of parabolic pulses in normal-dispersion fiber amplifiers," *J. Opt. Soc. Am. B* **19**, 461–469 (2002).
4. I. N. Duling III, "Subpicosecond all-fiber Erbium laser," *Electron. Lett.* **27** 544–545 (1991).
5. K. Tamura, E. P. Ippen, H. A. Haus, and L. E. Nelson, "77-fs pulse generation from a stretched-pulse mode-locked all-fiber ring laser," *Opt. Lett.* **18** 1080–1082 (1993).
6. K. Tamura, L. E. Nelson, H. A. Haus, and E. P. Ippen, "Soliton versus nonsoliton operation of fiber ring lasers," *Appl. Phys. Lett.* **64**, 149 (1994).
7. M. Hofer, M. E. Fermann, and L. Goldberg, "High power side-pumped passively mode-locked Er-Yb fiber laser," *IEEE Photonics Technol. Lett.* **10**, 1247–1249 (1998).
8. L. Lefort, J. H. V. Price, D. J. Richardson, G. J. Spohler, R. Pashotta, U. Keller, A. R. Fry, and J. Weston, "Practical low-noise stretched-pulse Yb³⁺-doped fiber laser," *Opt. Lett.* **27**, 291–293 (2002).
9. B. Ortaç, A. Hideur, T. Chartier, M. Brunel, C. Zkul, F. Sanchez, "90 fs generation from a stretched-pulse ytterbium doped fiber laser," *Opt. Lett.* **28**, 1305 (2003).
10. F. Ö. Ilday, J. R. Buckley, H. Lim, F. W. Wise, W. G. Clark, "Generation of 50-fs, 5-nJ pulses at 1.03 μ m from a wave-breaking-free fiber laser," *Opt. Lett.* **28**, 1365–1367 (2003).
11. J. Buckley, F. Ö. Ilday, F. W. Wise, and T. Sosnowski, "Femtosecond fiber lasers with pulse energies above 10 nJ," *Opt. Lett.* **30**, 1888 (2005).
12. F. Ö. Ilday, J. R. Buckley, and F. W. Wise "Self-Similar Evolution of Parabolic Pulses in a Laser," *Phys. Rev. Lett.* **92**, 213902 (2004).

13. M. E. Fermann, L.-M. Yang, M. L. Stock, and M. J. Andrejco, "Environmentally stable Kerr-type mode-locked erbium fiber laser producing 360-fs pulses," *Opt. Lett.* **19**, 43-45 (1994).
14. H. Lim, A. Chong, and F. W. Wise, "Environmentally-stable femtosecond ytterbium fiber laser with birefringent photonic bandgap fiber," *Opt. Express* **13**, 3460-3464 (2005), <http://www.opticsexpress.org/abstract.cfm?URI=OPEX-13-9-3460>.
15. I. Hartl, G. Imeshev, L. Dong, G. C. Cho and M. E. Fermann, "Ultra-compact dispersion compensated femtosecond fiber oscillators and amplifiers," CLEO, Baltimore, paper CThG1, May 2005.
16. www.batop.de
17. T. Clausnitzer, J. Limpert, K. Zöllner, H. Zellmer, H.-J. Fuchs, E.-B. Kley, A. Tünnermann, M. Jupé, and D. Ristau, "Highly efficient transmission gratings in fused silica for chirped-pulse amplification systems," *Appl. Opt.* **42**, 6934-6938 (2003).
18. M. Guina, N. Xiang, A. Vainionpää, O. G. Okhotnikov, T. Sajavaara, and J. Keinonen, "Self-starting stretched-pulse fiber laser mode locked and stabilized with slow and fast semiconductor saturable absorbers," *Opt. Lett.* **26** 1809-1811 (2001)

1. Introduction

Propagation of short optical pulses with high peak powers inside optical fibers can cause high pulse distortions, and pulse break-up due to high non-linearities inside the fiber. Inside mode-locked fiber lasers but also in amplifiers non-linearities are important due to the fact that the highest allowable total non-linear phaseshift is usually in the order of π or less, if the pulse is to be compressible afterwards. In [1] and [2] it was shown that parabolic pulses with linear chirp can be generated in high gain amplifiers. Such pulses can propagate self-similar - that is in a form preserving manner - inside fibers with normal dispersion and high gain, even if the total non-linear phaseshift exceeds π . As the pulse propagates, the temporal and spectral width increases exponentially, while maintaining a linear chirp, which can be removed afterwards. In [1] and [3] a wide range of different pulse shapes were shown to evolve asymptotically toward the parabolic shape, but dependent on the initial shape, longer or shorter lengths of fiber were needed for the pulse to converge.

Self-similar oscillators generating linearly chirped parabolic pulses are an interesting source for self-similar amplifiers, as the seed pulse from such an oscillator does not need a long section of fiber with gain to evolve into the parabolic pulse, and hence, self-similar amplifiers based on shorter fibers can be obtained.

The pulse evolution in a self-similar oscillator differs from pulse evolution in the well known soliton [4] and stretched pulse lasers [5]. In soliton lasers a pulse is generated which maintains an almost constant temporal width during one round trip: the soliton. A stretched pulse laser consists of two sections of fiber with normal and anomalous dispersion causing the chirp to change from positive to negative and back to positive during one round trip. In the self-similar laser, the chirp increases monotonically as the pulse propagates inside the fiber. There, the pulse is only compressed at points inside the laser where there are no nonlinearities affecting the pulse. Another important issue for a self-similar laser is that the pulse must experience a large gain per round trip with an initial almost exponential gain inside the gain medium in order to take advantage of the spectral bandwidth of the gain medium, to shape the pulse. The net cavity dispersion should also be positive so that the pulse is always positively chirped.

The energy achievable in soliton fiber laser systems is limited to some ten picojoules [6]. On the other hand, stretched pulse lasers with output energies from tens of picojoules to some nanojoules have been reported [7, 8, 9, 10]. Self-similar pulse evolution inside mode-locked fiber lasers has recently been shown to extend the obtainable pulse energy beyond the limit found in stretched-pulse lasers [11]. Therefore, the self-similar pulse regime is an interesting regime to investigate. However, so far, self-similar pulses have only been generated from fiber lasers based on the non-linear polarization evolution in the ring geometry [12]. This method does not allow the use of PM fibers because of the walk-off between light polarized along

the two axis of the fiber. Hence, environmentally stable lasers cannot be obtained with this geometry, as non-linear polarization evolution in non-PM fibers is sensitive to environmentally induced changes in the birefringence of the fiber.

Environmentally stable fiber laser have, however, been reported in a variety of other configurations, based on both nonlinear polarization evolution [13, 14] and saturable absorbers [15]. However, as environmental instabilities in fiber lasers mainly arise from environmentally induced changes in the birefringence of non-PM fibers, causing a change of the polarization evolution, the most natural approach is to use PM fibers with the light polarized only along the slow axis. This off cause eliminates the possibility of using non-linear polarization evolution.

2. Cavity design

In this paper we report on the generation of self-similar pulses from a linear cavity comprising only PM fibers. Two different cavity configurations have been investigated and self-starting self-similar pulses could be generated over a wide range of parameters such as output coupling, pump power and net cavity dispersion.

In Fig. 1, the two different cavity configurations can be seen. In both cases the mode-locking mechanism is based on a semiconductor saturable absorber mirror (SAM) and highly efficient transmission gratings have been used for intra cavity dispersion compensation. The fiber length inside the cavity was also chosen to be the same in the two cases, and the only difference was the choice of output coupling. In one case (Fig. 1(a)) the output coupler was a fixed fiber pig-tailed coupler allowing for a fiber based output. In the other case (Fig. 1(b)) the output coupler was based on a bulk polarizer and a quarter-wave plate allowing a tunable output coupling.

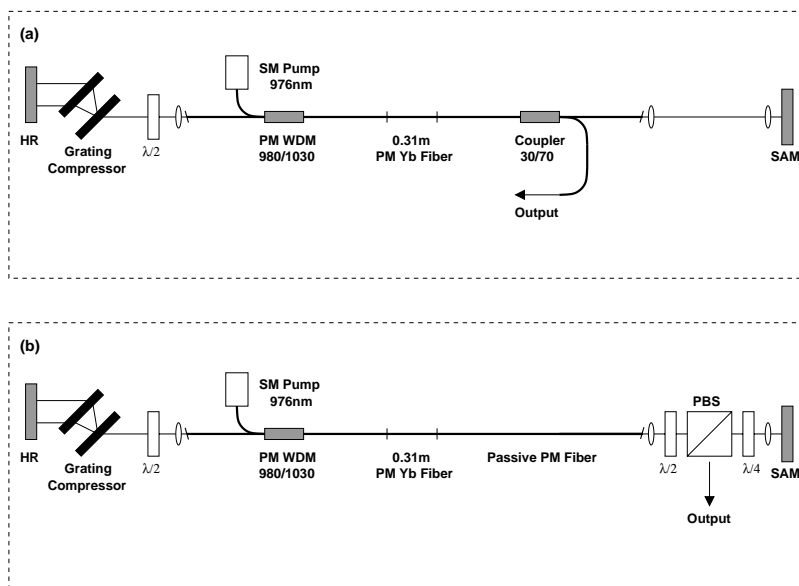


Fig. 1. The two different cavity designs: (a) with fiber output coupler and (b) with variable bulk output coupler. PM - polarization maintaining, HR - high reflection mirror, SAM - saturable absorber mirror, PBS - polarization beam splitter

The gain medium was a 31 cm long highly ytterbium doped (~ 300 dB/m absorption @ 976 nm) PM fiber with a mode-field diameter of $4.8 \mu\text{m}$. The utilization of the minimal length of gain fiber allows to decouple gain bandwidth filtering from the nonlinear evolution in the

undoped fiber because the effect of GVD and nonlinearity can be neglected during the amplification [12]. This fiber was pumped through a thin-film PM WDM by a single mode diode providing a maximum output power of 400 mW at a wavelength of 976 nm. The passive fibers used in the setup were Panda 980 PM fibers with mode field diameters of $\sim 7 \mu\text{m}$ @ 1035 nm and a dispersion of $\sim 0.024 \text{ ps}^2/\text{m}$. The total fiber length inside the cavity was 5.6 m for both cavity designs and in both cases the length of the passive fiber on both sides of the gain medium was equal in order to create symmetric conditions for the pulse evolution after the gain medium in both directions. All the PM fibers were fusion spliced together with an estimated polarization extinction ratio above 37.5 dB and all fiber ends were either angle polished or angle cleaved.

The SAM is commercially available [16], and is based on a non-resonant design, using a GaAs/AlAs Bragg mirror with 27 layer pairs and 26 low temperature molecular beam epitaxy grown InGaAs quantum wells in front of the mirror. The AR coated device has a low-intensity absorption of 45 %, a modulation depth of $\sim 30 \%$, and a saturation fluence of $\sim 100 \mu\text{J}/\text{cm}^2$. In a pump-probe experiment using 200 fs pulses, the recovery dynamics of the optical excitation has been measured. The SAM shows a bi-temporal impulse response with a short relaxation time of $< 200 \text{ fs}$ and a slower part of 500 fs. The ratio of the fast and slow parts has been determined to 3:2. To achieve the saturation threshold a telescope was used to image the output of the fiber onto the SAM.

The transmission gratings used for intra cavity dispersion compensation were 1250 lines/mm gratings made of fused silica [17] with a high transmission into first order ($>95\%$ @ 1035 nm). The gratings were set up in Lithrow angle (40°) with a grating separation of $\sim 16 \text{ mm}$. A half-wave plate was used between the gratings and the PM fiber to ensure excitation of only the slow axis. In the case of the bulk polarizer and the quarter-wave plate as an output coupler, an additional half-wave plate was also used to ensure excitation of only the slow axis of the fiber after the polarizer. If the axis of the fiber itself is properly aligned to the grating or the polarizer, the half wave plate can be removed resulting in an even simpler setup. With the fiber pig-tailed thin-film 30:70 PM coupler used in the other configuration, a half-wave plate was no longer necessary, as the coupler in it self worked as a polarizer transmitting only light in the slow axis.

3. Experimental results

Special care had to be taken to align the half-wave plates to ensure excitation of only the slow axis with a high extinction ratio. Especially in the setup with the bulk output coupler it was difficult to align the wave-plates accurately, as in this configuration there was no polarization dependent loss inside the fiber. With the fiber pig-tailed coupler/polarizer in the other setup it was much easier, as only one wave-plate had to be aligned. If the wave-plates were not perfectly aligned, smaller or larger ripples on top of the spectrum could be observed.

Self-similar spectra, characterized by a parabolic top and with steep edges [12], with a FWHM between 8 and 12 nm dependent on the pump power, could be obtained with a net cavity dispersion of $\sim 0.03 \text{ ps}^2$. A typical output spectrum is shown in Fig. 2, where the FWHM of the self-similar spectrum is 11.3nm. As the pump power was increased the spectral width increased monotonically, until the threshold for double-pulsing was reached (i.e. two pulses per round trip). The relatively large value of the net cavity dispersion of ($\geq 0.03 \text{ ps}^2$) is chosen to obtain a symmetric spectrum.

In contrast, for lower but still positive values of net cavity dispersion broader but asymmetric and more structured spectra could be observed, which correspond to the stretched-pulse regime [11]. In the following we will only focus on the self-similar regime.

The highest output pulse energy was obtained from the setup with the bulk output coupler, where the output coupling could be tuned. For a high output coupling coefficient the highest pulse energies of 1 nJ were obtained with a repetition rate of 17 MHz. The value of 1 nJ is

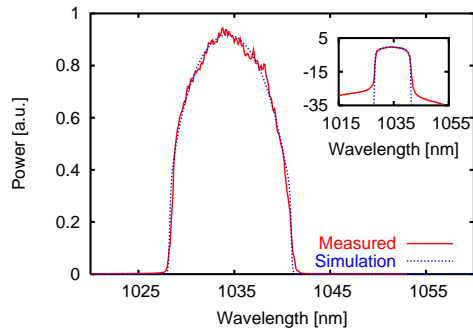


Fig. 2. Solid curve: Typical output spectrum on a linear scale of the laser operated in the self-similar regime (net cavity dispersion $\sim 0.03 \text{ ps}^2$). Dotted curve: numerical simulation. Inset: log. scale

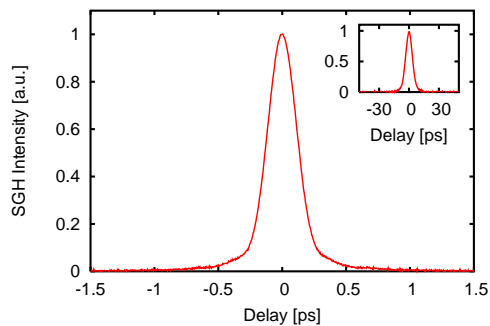


Fig. 3. Autocorrelation trace of the externally compressed pulse at a pulse energy of 1 nJ with an autocorrelation FWHM of 280 fs. Inset: Uncompressed output pulse with an autocorrelation FWHM of 8.2 ps.

smaller than what have very recently been obtained with a self-similar ring laser [11], where more degrees of freedom is available to optimize the output pulse energy. However fewer degrees of freedom highly simplifies finding the self-similar regime. In [11] the optimal pulse energy was also found to be highly sensitive to the cavity length, and it is expected, that higher pulse energy can also be obtained if the cavity length of this cavity is optimized.

The chirped self-similar output pulse had a duration of 7.2 ps (8.2 ps FWHM on the background free autocorrelator) (see Fig. 3), but could externally be compressed to an autocorrelation FWHM of 280 fs on the background free autocorrelator. The pulse duration can be calculated from the width of the autocorrelation by assuming a transform limited self-similar spectrum of the compressed pulse (deconvolution factor 1.33) and is evaluated to be 210 fs. From the actual measured spectrum a deconvolution factor of 1.65 is numerically calculated assuming no chirp. It shows that even if the experimental spectrum only slightly deviates from the parabolic shape as in our case, the deconvolution factor changes significantly. Thus, an even more optimistic pulse duration of 170 fs can be evaluated.

The scan range of the background free autocorrelator was 150 ps, but to check for multiple pulsing and to ensure that there was only a single pulse in the output, a 25 GHz photo diode in combination with a 50 GHz sampling oscilloscope providing a scan range from 30 ps to 60 ns has been used.

Self-similar spectra similar to the spectrum shown in Fig. 2 were also obtained from the setup with the fiber pig-tailed coupler. The output pulse energy was ~ 0.12 nJ, which could be externally re-compressed to an autocorrelation FWHM of 350 fs. Due to the fixed output coupling of 30%, which is lower than in the other setup, no flexibility was given to find the regime of higher pulse energy and shorter pulses. Additionally, an extra loss of 30% is introduced inside the cavity due to the fact that the coupler is passed in both directions. Nevertheless, by optimizing the outcoupling ratio it should be possible to obtain even better results with the advantage of an alignment-free fiber output.

To make sure the laser operates in the self similar regime some inspections have to be made. Firstly, the spectrum should of course exhibit a self-similar shape, which is fulfilled in our case. Secondly, an important condition for self-similar evolution is that pulse is always positively chirped inside the cavity, and with a minimum pulse duration after the intra cavity gratings just before entering the fiber [11]. The negative dispersion given by the grating pair used for external compression (~ -0.36 ps² (double pass)) was higher than of the pair used inside the cavity. In addition, only half the length of intra cavity fiber is passed before the pulse is coupled out, indicating that the pulse is still highly positively chirped before entering the fiber after the intra cavity grating pair. As the dispersion from this point on inside the cavity is positive until the pulse again reaches the intra cavity gratings, this point must be a minimum point. Hence, the pulse is not completely compressed during propagation inside the cavity and therefore maintains its shape. As an additional verification, a numerical simulation of the cavity was carried out. Each segment was treated separately by solving the nonlinear Schrödinger equation with the parameters of our experimental setup [12]. In Fig. 2 the simulated spectrum can be seen to be in good agreement with the measured spectrum. In the simulation the pulse exhibits self-similar pulse propagation [11] and is always positively chirped.

In both configurations the laser was self-starting and immediately jumped back into the same mode-locked state without any external perturbations if, for instance, switching the laser off and on again. It has previously been shown, that SAMs exhibiting a bi-temporal impulse response can fulfill both requirements of self-starting and symmetric spectra [18]. Furthermore, the use of PM fibers made the laser stable toward environmentally induced changes to the birefringence of the fiber. The fibers could be twisted and moved around while maintaining a stable mode-locked output. This was verified by observing a uniform train of pulses using a fast photo diode and an analog scope.

4. Conclusion

In conclusion, we have demonstrated, for the first time to our knowledge that a self-starting self-similar oscillator can be obtained with a linear cavity where a SAM is used as the nonlinear mode-locking mechanism. Further, the oscillator was intrinsically environmentally stable, as only PM fibers were used. Pulses with an energy of 1 nJ at a repetition rate of 17 MHz are obtained, where the pulse duration is characterized to be 7.2 ps. The self-similar spectral profile is centered at 1035 nm with a width of 11.3 nm. These pulses have been externally compressed to a pulse duration of 280 fs autocorrelation width.

Acknowledgments

We gratefully acknowledge D. Fischer and G. Steinmeyer, Max-Born- Institute, Berlin for carefully characterizing the SAM employed in the experiments. Furthermore, we would like to thank the Deutsche Forschungsgemeinschaft (DFG) under contract number RI650/11-1, for partly supporting the work and the NKT Academy for financing the Ph.d of C. K. Nielsen and T. Schreiber.